A combination of NO_x trapping materials and Urea-SCR catalysts for use in the removal of NO_x from mobile diesel engines.

James A. Sullivan* and Orla Keane,
UCD School of Chemistry and Chemical Biology,
Belfield,
Dublin 4,
Ireland.

Abstract

Preliminary studies on a series of nanocomposite BaO-Fe ZSM-5 materials have been carried out to determine the feasibility of combining NO_x trapping and SCR-NH_3 reactions to develop a system that might be applicable to reducing NO_x emissions from diesel-powered vehicles. The materials are analysed for SCR-NH_3 and SCR-urea reactivity, their NO_x trapping and NH_3 trapping capacities are probed using Temperature Programmed Desorption (TPD) and the activities of the catalysts for promoting the NH_{3ads} + NO/O_2 → N_2 and NO_{xads} + NH_3 → N_2 reactions are studied using Temperature Programmed Surface Reaction (TPSR).

Keywords: NO_x, NH_3, SCR, Urea, BaO.

Contact Details. James.Sullivan@ucd.ie, T + 353 1 7162135, F +353 1 7162127.

Introduction

The removal of NO_x from exhaust streams of a net oxidising nature such as stationary power sources, fuel-lean gasoline engine exhausts and diesel engine exhausts remains an intensively studied area of research within the heterogeneous catalysis community [1-7].

In the case of the stationary power sources SCR-NH_3, where NO_x (rather then O_2) is *selectively* reduced over catalyst with NH_3 as a reducing agent, is a technology used to deNO_x emissions [8,9]. This is possible under these conditions since (a) these facilities are by definition stationary and thus any problems with keeping a supply of $NH_{3(g)}$ on site are minimised and (b) the amount of combustion taking place within the power station and thus the amount of NO_x generated is generally constant (therefore the amount of NH_3 required to remove this NO_x is also constant). The dose of NH_3 to the reaction mixture is important since there must be sufficient NH_3 added to remove the NO_x but excess addition of NH_3 is undesirable. Any excess NH_3 over NO_x is either oxidised to N_2 or NO_x over the catalyst or oxidised to NO_x in the atmosphere if it "slips" beyond the catalyst, thereby rendering the entire process more expensive (if NH_3 is oxidised to N_2) or an entire waste of effort (if excess NH_3 is oxidised to NO_x).

The selective trapping of NO (via NO_2) onto BaO-containing materials followed by, once the trap is saturated, a reduction of $Ba(NO_3)_2$ and regeneration of BaO, using a pulse of hydrocarbons and CO (NO_x Storage and Reduction (NSR)) is a technique that has found application in lean-burn gasoline vehicles [10,11].

There are problematic issues associated with the former technique (SCR-NH_3) since NH_3 is a gas which is difficult to both store and dose to the exhaust. The latter point is important since the formation of NO_x from a diesel engine is not at a constant level (since driving conditions vary). The former problem can be resolved through the use of solutions of urea and a suitable hydrolysis catalyst (to form NH_3 on board the vehicle) but the latter problem requires a sophisticated NO_x sensor coupled to the urea delivery system to ensure correct dosage of NH_3 to the catalyst and such systems are, as yet, unavailable.

The latter technique (NSR) is also unsuitable for direct use on a diesel engine due to the fact that it is unable to deliver the pulse of CO and hydrocarbons which the lean-burn gasoline engine can deliver since, due to its particular 4-stroke cycle, a diesel engine is unable to run in a fuel-rich mode. However there are adjustments to the lean-burn gasoline NSR cycle that can be made in order to make it effective for the removal of NO_x from a diesel engine exhaust. One possibility would involve direct injection of the diesel (hydrocarbon) fuel over the catalyst while a second would be the on-board generation of H_2 and CO mixtures through on board reforming of the diesel by injection of the fuel into the combustion chambers directly following the fuel combustion step of the 4-stroke cycle [12, 13].

Here we propose one possible further method of removing NO_x emissions from the exhausts of diesel engines which is based on a combination of both of these approaches over a multi-component catalyst (Figure 1). Using this proposed technique a catalyst would consist of several components, each of which would have a specific function within the NO_x removal cycle. In particular the catalyst would consist of (a) BaO NO_x trapping sites, (b) hydrolysis sites to convert urea quantitatively into NH_3 + CO_2, (c) acid sites to trap any excess NH_3 and prevent NH_3 slip and (d) redox active sites to catalyse the NO + NH_3 reaction.

Specifically the cycle would operate as follows;

Beginning with the "clean" composite material

(a) Gaseous NO_x would be trapped on the material as $Ba(NO_3)_2$. This process would continue until the BaO is fully saturated. As is known, [10] the first step in $Ba(NO_3)_2$ formation from NO is the oxidation of NO to NO_2. We would envisage that this function would be carried out by either the exchanged Fe cations [14] or any external FeO crystallites.

(b) Urea would be <u>periodically</u> injected over the material. This would hydrolyse to NH_3+CO_2 with the NH_3 going on to reduce this $Ba(NO_3)_2$ to BaO+N_2+H_2O.

(c) Any excess NH_3 formed would be trapped on the acid sites as NH_4^+ (or NH_{3ads}) preventing NH_3 slip. This would offer a certain amount of "buffer" capacity to the dosage of urea (NH_3) to the catalyst to compensate for the changes in [NO] formed under transient operation conditions, *i.e.* the dosedoes of urea would not have to be as accurate as would be required in a straightforward SCR-NH_3 (or SCR-urea) deNO_x system.

(d) Gaseous NO_x would now have two possible courses of reaction, *i.e.* either reacting with the adsorbed NH_3 ("cleaning" the NH_3-covered acid sites and forming N_2) or reacting with the "clean" BaO to form $Ba(NO_3)_2$, essentially restarting the cycle.

We have tested various aspects of this cycle on composite materials using Ba containing Fe ZSM-5 catalysts as model materials. The Fe ZSM-5 portion of the composite material should possess SCR-NH_3 activity [15-17] (through redox active Fe ions) and NH_3-trapping capacity (through zeolitic acidity) while BaO (incorporated either as ion exchanged or wet impregnated Barium) should provide the NO_x trapping functionality [10-13].

Previous work within the group [18] has shown that urea solutions are not direct replacements for $NH_{3(g)}$ in terms of comparing the activity of a given catalyst for the SCR-NH_3 reaction and the SCR-Urea reaction. This effect is not due to the presence of H_2O in the reaction stream (urea is dosed to the catalyst in an aqueous solution) since several sets of catalysts that proved active for deNO_x under wet SCR-NH_3 conditions show no activity in the SCR-urea reaction [19]. This suggests that the urea in these conditions is not hydrolysing to form NH_3 (via a HNCO intermediate [20]) as would be expected but rather is either oxidising to N_2 or is reacting through some other path.

Other work [21] has shown that Fe ZSM-5 catalysts can retain a large amount of activity in the SCR-Urea reaction provided that the counter ion of the parent zeolite is Na^+ rather than NH_4^+. It is thought that in catalysts that are prepared with Brønsted acidity these acid sites promote the formation of melamine layers through the reaction of HNCO (an intermediate in urea decomposition to NH_3) with NH_3 [22].

The analysis has involved Temperature Programmed SCR activity using both NH_3 and urea as reducing agents, NO_x and NH_3 Temperature Programmed Desorption and Temperature Programmed Surface Reactions (using pre-adsorbed NO_x and NH_3) .

Experimental

Catalyst Preparation:

Fe ZSM-5 (0.8% Fe) and Ba ZSM-5 (4.3% Ba) were prepared by conventional ion-exchange method using Na-ZSM-5 (SiO_2/Al_2O_3 = 27) obtained from Schwandorf. A quantity of 1.0 g zeolite was shaken for 2 h in 100 ml of either 0.01M $FeSO_4.7H_2O$ or 0.01M $Ba(C_2H_3O_2)_2$. The samples were filtered, washed in hot (80 °C) deionised water, dried at 110 °C and calcined at 500 °C for 2 h.

Two composite catalysts containing Fe and Ba (Fe Ba ZSM-5) were prepared using the Fe ZSM-5 prepared above followed by the introduction of Ba by both ion-exchange (ie) and wet impregnation (wi) techniques. The former catalyst was prepared first and subsequently the latter wass prepared to contain the same [Ba]. These materials contain 0.8% Fe and 1.7% Ba. The elemental compositions of each sample were determined by Atomic Absorption following acid digestion. All samples were pressed and sieved to particle sizes of 212-600 μm before use. Before TPD and TPSR experiments, each catalyst sample was outgassed at temperature 500 °C for 5 h in a flow of He in order to decompose $BaCO_3$ which forms following contact between

BaO and CO_2. Previous studies have shown that such an extended treatment at 500 °C in He is sufficient to decompose all the $BaCO_3$ [23].

Activity Studies:

The catalyst (10 mg) was held in a tubular quartz reactor using plugs of quartz wool. The reactants were blended using electronic mass flow controllers from cylinders of 1% NO and 1 % NH_3 in He (BOC Special Gases), O_2 and He (BOC) to give a reaction mixture of [NO] = 1000 ppm, [NH_3] = 1000 ppm, and [O_2] = 13% in a total flow of 100 ml/min. Solutions of urea were introduced into a heated zone before the reactor from a calibrated syringe driver. Aqueous solutions of 2.9 % urea were used at liquid flow rates that gave 940 ppm urea in the final reaction mixture. The reactions (SCR-NH_3 and SCR-urea) were studied under temperature-programmed conditions with a ramp rate of 10 °C min^{-1} between either 50 °C and 500 °C (SCR-NH_3) or 100 °C and 500 °C (SCR-urea). Levels of NO_x were continuously analysed, following suitable dilution, using an Advanced Pollution Instrumentation Inc. Nitrogen Oxides Analyser (Model 200) connected to a PC.

Temperature Programmed Desorption:

Catalyst acidity and interaction with NH_3 were probed using Temperature Programmed Desorption (TPD) of NH_3. The catalyst (50 mg) was dosed with NH_3 (1538 ppm) at 100 °C for 1 h. The NH_3 was then removed from the stream and the catalyst cooled to 50 °C in a flow of He. It was held at this temperature for 20 min and then the temperature was ramped from 50 to 500 °C at a ramp rate of 20 °C min^{-1}.

The NO_x-storage capabilities of the catalysts were probed using TPD of NO. The catalyst (50 mg) was dosed with NO (1538 ppm) and O_2 (19% O_2) at 400 °C for

2 h and cooled to 100 °C in this flow. The NO and O_2 were removed from the stream using an electrically actuated valve and replaced with an equivalent flow of He. The catalyst was cooled to 50 °C. Once the NO signal returned to a baseline level the temperature was ramped from 50 °C to 750 °C at a rate of 20 °C min^{-1}. In some experiments the samples were dosed at 100 °C.

Temperature Programmed Surface Reaction:

NH_3-TPSR experiments were carried out by exposing the sample (50 mg) in NH_3 according to the procedure applied in the NH_3-TPD measurements. The reactor was then purged in a flow of He and cooled to 50 °C. The catalyst was then heated to 500 °C at a temperature ramp rate of 20 °C min^{-1} in a flow of 1859 ppm NO and 1.7% O_2.

NO-TPSR experiments were carried out by exposing the sample (50 mg) to NO_x according to the procedure applied in the NO-TPD measurements. The reactor was purged in a flow of He and subsequently NH_3 (1538 ppm) switched over the catalyst. Once the NH_3 level reached a stationary value, the temperature was ramped from 100 °C to 750 °C at a rate of 20 °C min^{-1}. Similar experiments were also carried out heating the catalyst in a flow of both NH_3 (1538 ppm) and O_2 (1.8%).

In all cases (NH_3-TPD, NO-TPD, NH_3-TPSR and NO-TPSR) the effluent gas was continuously monitored by mass spectrometry (Prolab Residual Gas Analysis) with the gas phase being introduced to the Prolab via a heated and continuously evacuated capillary. The mass spectrometer monitors masses at 18, 17, 16 and 15 (H_2O, NH_3 and various fragments of each), 28 (N_2, CO), 30 (NO), 32 (O_2) and 44 (CO_2, N_2O) as a function of temperature. The data are then corrected for overlapping masses (e.g. the contribution of the H_2O fragment at 17 to the NH_3 signal was removed) [24].

Results and Discussion.

Obviously considering the processes covered in Figure 1 it is essential that the composite material is active in the SCR-NH_3 reaction. Figure 2 shows the activity of the catalysts in the SCR-NH_3 reaction under temperature programmed conditions. It is clear that both the Na ZSM-5 parent zeolite and the ion exchanged Ba ZSM-5 material show little activity for this reaction. Previously under these reaction conditions, *i.e.* in the SCR-NH_3 reaction [20] a Na ZSM-5 catalyst which had been ion-exchanged in a solution of HNO_3 showed a certain amount of activity for the SCR-NH_3 reaction at temperatures above 400 °C. This suggests that Brønsted acidity promotes this SCR-NH_3 reactivity.

The Fe ZSM-5 material shows similar activity to other similarly prepared samples with deNO$_x$ activity commencing above 300 °C while the composite catalysts containing both Ba and Fe show similar profile shapes but with decreased deNO$_x$ activity. Thus it seems that the presence of Ba poisons the activity of the Fe ions within the zeolite to a certain extent. Surprisingly the ion-exchanged barium catalyst shows a greater decrease in activity relative to the Fe ZSM-5 than the wet impregnated sample. This suggests that a simple channel blocking mechanism is not the only factor responsible for the decreased activity of Fe ZSM-5 (as it would be expected that wet impregnated BaO would block pores possibly preventing the reactants from reaching the active sites within the zeolite).

Considering the cycle above, the activity of the material in the SCR-urea reaction also becomes important (but not vital). If the materials do possess SCR-urea activity then there would be no need to provide a separate urea hydrolysis catalyst and the urea could be dosed directly onto the catalyst at the appropriate point of the cycle. However, if the catalysts have no, or limited, SCR-urea activity then a secondary hydrolysis catalyst or system would be required to form NH_3 which can go on to react over the catalysts in the SCR-NH_3 reaction.

Previous work [21] has shown that the presence of H_2O on these and related catalysts has little effect on SCR-NH_3 reactivity. To provide a more realistic picture of how the change in reductant from gaseous NH_3 to aqueous urea affects SCR-NH_3 reactvity, then the SCR-NH_3 experiments should be carried out in the presence of both H_2O and $CO_{2\,(g)}$. However, it is not envisaged that the presence of the relatively small amounts of CO_2 that would be formed from the decomposition of urea would have major effects on the overall deNO$_x$ activity.

Figure 3 shows the activity of the four materials in the SCR-urea reaction. The deNO$_x$ activity of the Fe ZSM falls to roughly half of the levels of activity seen in the SCR-NH_3 reaction in Figure 2. This is in contrast to what has been seen previously where such catalysts retained a significant portion of their SCR-NH_3 activity under SCR-urea reaction conditions. However, the reaction conditions in the current work are slightly more challenging with less urea available for NO$_x$ reduction. Similarly the Fe Ba ZSM-5 (ie) catalyst shows a dramatic decrease in deNO$_\text{x}$ activity and is now no more active than the Ba ZSM-5 material. Interestingly the activity of the wet-impregnated composite catalyst (which was the least active of the Fe-containing materials in the SCR-NH_3 reaction) remains unchanged when urea is used as a reductant.

In conclusion, even though the catalysts have a relatively good SCR-NH_3 activity – and this activity is for the most part retained in the presence of H_2O, these results suggest that the materials are not sufficiently active in the SCR-urea reaction and that a separate urea hydrolysis reactor would be required in order for these materials to be effective in the cycle presented above.

The NO_x–trapping capacity of the materials is obviously important when the above cycle is considered since materials that can reversibly adsorb large amounts of NO_x would allow less frequent catalyst regeneration steps (urea / NH_3 dosages). We have measured the NO_x trapping capacity of the materials using NO_x-TPD.

Figures 4 and 5 show the Temperature Programmed NO_x desorption profiles. Figure 4 shows the profile seen over the Na ZSM-5 catalyst following dosages in NO/O_2 at both 100°C and 400 °C. There is a dramatic difference in the profiles seen in each case. The catalyst which had been dosed at 100 °C shows peaks at relatively high temperatures (400 °C and 600 °C) while the catalyst which had been dosed at 400 °C (and cooled in NO/O_2 to 100 °C) showed similar peaks as well as a large peak at 180 °C. This suggests that the treatment at 400 °C in NO/O_2 has created new NO_x adsorption sites on the catalyst surface that desorb NO_x at lower temperatures. These new sites may have been formed from dehydroxylation of the zeolite during the higher temperature dose. The previous work on Fe ZSM-5 zeolites [21] has shown the production of water during a temperature ramp, peaking at a temperature of 450 °C – commensurate with the dehydroxylation of the zeolite at this temperature. Thus, these results can be explained by the formation of sites on the catalyst surface through an extended treatment in NO/O_2 at 400 °C, which are populated with a weakly coordinated (nitrite-type) surface NO_x species while the sample is cooled from 400 °C to 100 °C.

However, it should be recalled that samples had all been outgassed in He at 500 °C before both doses. This suggests that either the new sites are created from an oxidation rather than a dehydroxylation or that the dehydroxylated sites are simply rehydroxylated during the dose at 100 °C through reaction with water impurity in the He carrier gas. Further work is ongoing to clarify this point.

Figure 5(a) shows the NO_x desorption profiles from the Fe ZSM-5, Ba ZSM-5 and the composite catalysts (and Na ZSM-5 for reference). In these experiments all the catalysts were dosed at 400 °C and then cooled to 100 °C in a flow of NO/O_2 in order to generate and populate the sites discussed above in which a form of NO_x is adsorbed that is unstable at temperatures above 200 °C.

The Fe ZSM-5 catalyst shows two desorption peaks at 150 °C (usually ascribed to the decomposition of a nitrite-type species) and 375 °C (usually ascribed to the decomposition of a nitrate-type species) [25] The temperature of these desorptions is slightly lower than the equivalent peaks on the ion exchanged Ba ZSM-5 catalyst (125 °C and 425 °C). This indicates that the NO_x adsorbed on the latter catalyst is more stable in both adsorbed configurations.

Both of the Fe Ba ZSM-5 composite materials show profiles that are equivalent to one another with two peaks at 180 °C and 390 °C. This shows that the method of incorporating Ba into the composite material does not affect the nature of the NO_x adsorption onto the catalyst. The nitrate-type species are less stable than the equivalent species on the Ba ZSM-5. This suggests that the presence of the Fe within the zeolite catalyses the decomposition. Exchanging metal ions into the ZSM-5 lattice removes the NO_x adsorption sites upon which NO_x is stable at the highest temperatures (600 °C) on Na ZSM-5. These temperatures of NO_x desorption are lower than those seen over other Ba-containing catalysts such as $CuBa/Al_2O_3$ [26] and this suggests that the adsorbed NO_x is less stable over these zeolitic materials than on the above-mentioned oxides.

Figure 5(b) is a histogram showing the total amount of NO_x and the NO_x associated with nitrite-type and nitrate-type decompositions produced from each of the catalysts during the NO_x TPD experiments. These show that (as expected) the Na ZSM-5 material adsorbs more NO_x when dosed at 400 °C rather than at 100 °C and that all the increase in NO_x adsorbed is due to the formation of nitrite-type species.

Overall more NO_x is adsorbed on the Ba ZSM-5 material than on the parent zeolite while less is adsorbed on the Fe ZSM-5 catalyst. The composite materials adsorb intermediate amounts of NO_x.

Interestingly, exchanging Fe into the samples decreases the total amount of NO_x that the materials can adsorb. This might be due external FeO-type crystallites blocking access to internal Fe or Na ions or framework NO_x adsorption sites..

As mentioned above the composite materials behave in almost exactly the same manners as one another not only in terms of the temperatures of maximum desorption (above) but also in terms of the overall amount of NO_x desorbed and the distribution of types of surface species formed.

In terms of overall NO_x storage these materials adsorb far less NO_x than standard $Pt/Ba/Al_2O_3$ materials, e.g. Forzatti et al. [11] record a NO_x storage of ~1500 $\mu mol\ g^{-1}$ of material (compared to ~470 $\mu mol\ g^{-1}$ for our Ba ZSM-5 catalyst) following a treatment in NO and O_2 containing gases. However, it must be recalled that this is not a direct comparison since their materials contain ~ 16 % Ba while the materials we are studying contain between 1.7 and 4.3% Ba.

The amounts of NO_x adsorbed on the composite catalysts is not a simple addition of the amounts of NO_x adsorbed on the individual single metal catalysts. This shows that there is some interference between the Fe and Ba species and the zeolite framework which prevents as much NO_x adsorbing onto the catalyst as there are sites available.

In conclusion these NO_x TPD experiments show that it is possible to store NO_x on these materials – a feature that is obviously necessary for the cycle presented in Figure 1 to be of use. We also need to know the reactivity of this NO_x in the presence of NH_3 since the cycle above requires that the $Ba(NO_3)_2$ formed during NO_x storage be converted to BaO upon contact with NH_3, and that the NH_3 and NO_2 released from the $Ba(NO_3)_2$ form N_2.

Figure 6 (a-d) shows the NO_x TPSR profiles where the catalysts are dosed in NO_x and then the temperature is ramped in a flow of NH_3 to 700 °C. These profiles show whether it is possible to regenerate the BaO from $Ba(NO_3)_2$ using NH_3 as a reducing agent. This step is vital in the cycle presented in Figure 1. Previously such BaO NO_x traps have been regenerated using CO, H_2 or hydrocarbon reductants [10-13].

A large desorption of NH_3 was noted from all the materials during the temperature ramp in NH_3 – showing that NH_3 can adsorb to a large extent over the NO_x treated surfaces. This shows that there are sites available on the surface that are accessible to NH_3 that it is not possible to cover with NO_x. It is also possible that during this experiment the NH_3 is adsorbed *on* the adsorbed NO_x. To a first approximation more NH_3 is actually desorbed during these experiments than is seen during the NH_3 TPD experiments presented later (Figure 7(a)), suggesting the creation of some surface adsorption sites for NH_3. Quantitative analysis of the difference is not possible since there is a purge period during the latter experiments during which weakly adsorbed NH_3 is removed while this is not the case here.

Over Fe-containing catalysts (from which two peaks were observed during the NO_x TPD above) there is very little desorption of NO_x over the entire temperature range of the experiment because the adsorbed NO_x reacts with (either adsorbed or gaseous) NH_3 to form large amounts of N_2. At higher temperatures the NH_3 itself reacts with some surface oxygen species to form N_2.

Over all the Fe-containing catalysts the main production of N_2 is seen in one peak at ~ 300°C. This temperature is intermediate between the two decompositions of nitrite and nitrate on the catalyst surface (Figure 5(a)). It is interesting that there is neither NO_x desorption nor N_2 production at temperatures at which the nitrite-type species was seen to decompose (~200 °C) during the NO_x TPDs above. This suggests that either the presence of NH_3 stabilises the nitrite against decomposition (possibly through the formation of a surface complex) or that this nitrite-type species reacted with NH_3 to form N_2 during the dose in NH_3 at 100 °C prior to the commencement of the temperature ramp. Further studies are ongoing to elucidate this point.

Small amounts of N_2O are seen from the Ba-containing composite materials as well as the main N_2 peak but again desorption of NO_x was minimal. More N_2 is formed during TPSR over the Ba Fe ZSM-5 (ie) sample even though both composite materials have similar concentrations of $NO_{x\ \mathrm{ads}}$.

The Ba ZSM-5 material is not as effective a catalyst for the formation of N_2 from this reaction (Figure 6(b)). The temperature of N_2 production is significantly higher, there is far more N_2O formed and there is also a significant amount of NO_x desorbed as the temperature is raised. This shows that for efficient N_2 production under the previous TPSR conditions some redox active sites are required.

These experiments have also been carried out with the NO_x-dosed catalysts being ramped in NH_3 / O_2 mixtures and similar results have been noted. The latter experiments also show the reaction between NH_3 and O_2 at higher temperatures over all materials and an extra formation of N_2 at ~ 150 °C (possibly from reaction of the nitrite-type species with NH_3) over the FeZSM-5 material (results not shown).

In conclusion these results clearly show that it is possible to react trapped NO_x with NH_3 to form N_2 (and N_2O) and also that in the presence of NH_3, NO_x will not simply desorb from Fe-containing catalysts without reaction, but rather react with NH_3 to form N_2.

The NH_3-handling characteristics of the proposed material are also of interest. Important features of the cycle presented above include the ability of the proposed materials to trap any excess NH_3 that is formed from the decomposition of urea and also to catalyse the reaction of this NH_{3ads} with gaseous NO_x. For this reason a series of Temperature Programmed NH_3 Desorption experiments (to measure NH_{3ads} stability) and Temperature Programmed Surface Reaction experiments (to measure the reactivity of NH_{3ads} towards $NO_{(g)}$) were carried out.

Figure 7(a) shows the NH_3 desorption profiles seen from each catalyst. The amounts of NH_3 desorbed during each TPD are shown in parentheses in the figure legend. It can be seen that all materials adsorb NH_3 and that there is a range of adsorption enthalpies over each catalyst. All the material samples show at least two distinct desorptions (generally one peaking between 150 °C and 250 °C and the second showing maximum NH_3 desorption between 250 °C and 350 °C) showing that there are two distinct sites (with different adsorption enthalpies) upon which NH_3 can adsorb. These peaks are least resolved from the Ba ZSM-5 material. The Na ZSM-5 and Fe ZSM-5 materials behave similarly to one another in terms of the positions of peak maxima although it does seem that there is a higher concentration of more strongly binding sites on the Na ZSM and a higher concentration of more weakly bonding sites on the Fe ZSM-5. The two composite materials (Fe Ba ZSM-5) also show similar NH_3-handling characteristics to one another showing that the mode of addition of the Ba does not affect the bonding between NH_3 and the resultant material. This was also the case when these materials were considered in the NO_x TPDs above. Generally desorption of NH_3 from these catalysts is at lower temperatures (and thus the NH_3 is less strongly bound to these catalysts) than from the Na and Fe ZSM-5.

In terms of the overall NH_3 storage capacity of these materials there is little difference between any of the combinations. Fe ZSM-5 adsorbs the most NH_3 while the parent Na ZSM-5 adsorbs the least. The addition of Ba to the Fe ZSM-5 decreases the overall concentration of NH_3 adsorption sites by about 30% and in terms of the absolute concentration of sites available (as well as the stability of these sites – see above) it is clear that the mode of addition of the Ba is not overly important.

In conclusion , from the viewpoint of the cycle presented in Figure 1 it is clear that all the materials studied will trap NH_3 and that a portion of this NH_3, to greater or lesser extents, will be transiently stable (and thus “trappable”) at temperatures above 300 °C.

Figure 8 (a-d) shows the TPSR profiles from these catalysts when they are dosed in NH_3 and subsequently ramped in a flow of NO/O_2. This reactivity is important in the final step of the cycle where the acidic sites are cleared of $NH_{3\ ads}$ (and incoming NO_x is reduced to N_2) and the cycle can recommence.

There are several features of these profiles common to each catalyst. The signals relating to NO show similar behaviour here to those relating to NH_3 in the previous TPSR experiments, *i.e.* an initial desorption as the temperature is raised (suggesting that there is a certain amount of NO_x adsorption on the NH_3-covered surfaces at 50 °C), followed by a decrease in gaseous NO_x concentration mirrored by a production of N_2 (as $NO_{(g)}$ reacts with NH_{3ads} → N_2). Once the surface is cleansed of $NH_{3\ ads}$ the NO level returns to its dose value of ~1859 ppm.

These profiles are very similar to one another over the Fe-containing materials but the Ba ZSM-5 catalyst shows a smaller NO_x desorption and a smaller gas phase NO_x reaction than the other catalysts.

The profiles for the production of N_2 show takes place in two stages peaking at ~100 °C and ~300 °C. As mentioned above the former peak is accompanied by a desorption of NO_x from the surface (as seen by an increase in the $NO_{x(g)}$ levels) while the latter is accompanied by a decrease in the gaseous NO_x concentration. This suggests that the former production of N_2 arises from a surface NO/NH_3 complex while the latter arises from an interaction between $NO_{(g)}$ and NH_{3ads}.

There is also an elevated level of N_2 at the beginning of the experiment (50 °C). This suggests that the reaction between adsorbed NH_3 and NO can also proceed at lower temperatures.

The amounts of N_2 formed during each of these events (lower temperature NO_{ads}+$NH_{3\ ads}$ and higher temperature $NO_{(g)}$ + NH_{3ads}) differs as a function of catalytic material *i.e.* more N_2 is formed during the high temperature event over the Fe ZSM-5 and the Fe Ba ZSM-5 (wi) catalysts while more is formed during the low temperature event over the Ba ZSM and the Fe Ba ZSM-5 (ie) catalysts.

The ratios of these N_2 productions does not seem to be directly related to the concentrations of adsorbed NH_3 seen in the previous TPD experiments (Figure 7) or indeed to the different amounts of high temperature stable and low temperature stable NH_3 seen in those experiments.

The fact that some lower temperature production of N_2 is also seen during the dose with NO suggests that the amounts of N_2 formed during the lower temperature event may be related to the length of the dose at 100 °C in $NO_{(g)}$.

These profiles also differ from those seen in the reverse experiment (figures 6 a-d) in that there was a significant amount of N_2O formed over each catalyst. This, confirming what we have presented above, suggests different reaction pathways for the $NO_{x\text{ads}}$+$NH_{3(g)}$ and the $NH_{3\text{ads}}$+$NO_{x(g)}$ reactions. The N_2O formed at two temperatures (~200 °C and ~350 °C) over the Fe-containing catalysts. Roughly equivalent amounts were formed over the Fe ZSM-5 and the Fe Ba ZSM-5 (wi) with relatively minor amounts being formed over the Ba Fe ZSM-5 (ie) material. Over the Ba ZSM-5 there is a continuous production of N_2O between 150 and 450 °C (recall there was also significant N_2O production over this material in the reverse experiments).

Thus we can say that over the Fe containing catalysts the production of N_2O is promoted in the presence of gas-phase NO. Similar results relating to the surface pathway to N_2O (albeit from NO + H_2 mixtures) have been noted over Pt/SiO_2 catalysts [27].

Finally during these experiments there is also a significant amount of un-reacted NH_3 desorbed from all the catalysts with the most arising from the Ba ZSM and wet impregnated composite catalysts. This is another difference between this reaction and the former TPSR experiments where there was no desorption of the pre-adsorbed NO_x from any of the Fe-containing materials.

In conclusion this final set of results clearly show that it is possible to (a) trap NH_3 on these materials and (b) react this adsorbed NH_3 with gaseous NO_x to form N_2 (and N_2O) thus filling an important criterion for the cycle proposed in Figure 1.

However one feature of these experiments that may count against the overall process is that at relatively low temperatures it is possible to remove NH_3 from the catalyst and not react it with NO_x but rather it is able to "slip" through into the gas phase.

Conclusions.

We have shown that it is possible to combine basic NO_x trapping BaO species with redox active Fe ions within an acidic zeolite to generate a material that can carry out all the tasks necessary to remove NO_x from the exhaust of a diesel powered vehicle using the cycle portrayed in figure 1. These include trapping NO_x, trapping NH_3 and catalysing both the NO + NH_3 SCR reaction as well as to varying extents the NO_{ads} + NH_3 and NH_{3ads} + NO reactions.

Catalysts that are active for the SCR-NH_3 reaction are generally less active for the SCR-urea reaction. This suggests that in order for the above reaction scheme to be operative in real conditions a separate urea hydrolysis system which would quantitatively convert urea to NH_3 would be required.

The presence of Ba with Fe within a ZSM-5 framework increases the NO_x adsorption capacity and decreases the NH_3 adsorption capacity. This is as expected as a basic material is added to the Fe ZSM-5. The presence of Ba also decreases the SCR-NH_3 activity of the materials but has relatively minor effects on transient surface reaction activities (both NO_{xads} + $NH_{3(g)}$ and NH_{3ads} + $NO/O_{2(g)}$).

The latter transient results showed generally encouraging results in terms of activity and selectivity as they showed that it was possible to react adsorbed NO_x (and presumably $Ba(NO_3)_2$) with NH_3 and form N_2. Thus it is clear that it is possible to regenerate NO_x traps using NH_3 and (at temperatures > 300 °C) react excess NH_3 with $NO_{(g)}$.

As well as clarifying the nature of the NO_x adsorption sites that form on ZSM-5 following treatment at 400 °C (figure 4) and the fate of nitrite-type species on the catalyst surface in the presence of NH_3 at relatively low temperatures (figures 6 a-d), future work will involve analysing the materials under conditions approaching those under which such a system would be expected to operate. This would involve trying to operate the system under isothermal conditions with transient injections of urea into a stream of NO / O_2 while monitoring the exit NO gas concentration. In order for this to be an effective cycle however, a component will need to be added which will catalyse the urea decomposition. Once such a system is found (and TiO_2 has recently been reported as a material likely to promote urea→ NH_3 [28]) this series of experiments will be carried out.

Acknowledgements: We would like to acknowledge the Irish Research Council for Science, Engineering and Technology for support of this work under grant number SC/02/227. The Faculty of Science UCD is also gratefully acknowledged for the provision of a start-up grant. We also thank Julie Doherty for performing preliminary experiments.

References

1 K.C. Taylor, Catal. Rev. Sci. Eng. 35, (1993) 457.

2 M. Iwamoto, K. Yahiro, Tanda, N. Mizuno, Y. Mine, S. Kagawa, J Phys. Chem. 95 (1991) 3727.

3 R. Burch, J.P. Breen, F.C. Meunier, Appl. Catal., B: Env. 39, (2002), 283

4 N.W. Hayes, R.W. Joyner, E.S. Shapiro, Appl. Catal. B: Env., 8, (1996) 343.

5 R. Burch, Catal. Today, 26, (1995), 97.

6 Y. Li, J. Armor, Appl. Catal. B: Env. 2, (1993) 239.

7 M.C. Kung, H.H Kung,. Top. Catal. 10, (2000), 21.

8 H. Bosch, F. Janssen, Catal. Today. 2, (1998), 4.

9 R.M. Heck, Catal. Today. 53, (1999), 519.

10 P.Broqvist, H.Grönbeck, E.Fridell, I.Panas, Catal.Today 96, (2004), 71.

11 L.Letti, P. Forzatti, I.Nova, E.Tronconi, J.Catal., 204, (2001), 175

12 R.L.Muncrief, K.S.Kabin, M.P.Harold, AIChe, J, 50, (2004), 2526-2540

13 R.M. Petkar, C.A. Kardile, P.V. Deshpande, R. Soorajith, SAE (2005), sp-1974.

14 R.Giles, N.W.Cant, M.Kogel, T.Turek, D.L.Trimm, Appl. Catal. B: Env., 25 (2000), L75-L81.

15 L.J.Lobree, I.C.Hwang, J.A.Reimer, A.T.Bell, J.Catal., 186, (1999), 242.

16 R. Q. Long, R.T. Yang, J.Catal., 198, (2001), 20.

17 G. Qi, R.T. Yang, Appl. Catal. B: Env (in press)

18 J.A.Sullivan, J.A.Doherty, Appl. Catal. B: Env. 55, (2005), 185.

19 J.A.Doherty, MSc Thesis, UCD, (2004).

20 M. Koebel, M. Elsener, G. Madia, Ind. Eng. Chem. Res., 40, (2001), 52.

21 J.A.Sullivan, O.Keane, Appl.Catal.B: Env. 61, (2005), 244.

22 A.Satsuma, A.D.Cowan, N.W.Cant, D.L.Trimm, J.Catal., 181, (1999), 165.

23 J.A. Sullivan and, O.Keane, unpublished results, (2004).

24 Eight Peak Index of Mass Spectra, 3rd Edn., Unwin Brothers, Surrey, 1983.

25 V.A. Sadykov, S.L. Baron, V.A. Matyshak, G.M. Alikina, R.V. Bunina, A.Ya. Rozovskii, V.V. Lunin, E.V. Lumina, A.N Kharlanov, A.S. Ivanova, S.A. Veniaminov, Catal. Letts. 37 (1996) 157.

26 F.Prinetto, G. Ghiotti, I. Nova, L. Lietti, E. Tronconi, E. P. Forzatti. J. Phys.Chem. B. 105, (2001), 12732.

27 J.A.Sullivan, R. Burch and A.A. Shestov, Trans. IChemE, 78, (2000), 947.

28 P.Hauck, C.Gondalyia, A.Jentys, J.A.Lercher, Kinetics aspects of the urea-SCR Process. 4th International Conference on Environmental Catalysis, Heidleberg, June 2005, p9.

Figure Legends

Figure 1: Cycle showing the combination of a NO_x trapping material and an SCR-NH_3 catalyst for use in a proposed deNO_x system for mobile diesel engine exhausts.

Figure 2. Temperature Programmed SCR-NH_3 reaction. Na-ZSM-5 (□), Ba-ZSM-5 (◇), Fe Ba ZSM-5 (wet impregnated) (○), Fe Ba ZSM-5 (ion exchanged) (●) and Fe-ZSM-5 (◆).

Figure 3. Temperature Programmed SCR-urea reaction. Fe-ZSM-5 (◆), Fe Ba ZSM-5 (wet impregnated) (○), Ba-ZSM-5 (◇) and Fe Ba ZSM-5 (ion exchanged) (●).

Figure 4: NO_x TPD profiles from Na ZSM-5 which had been dosed with NO/O_2 at 100 °C (◆) or dosed in NO/O_2 at 400 °C and then cooled to 100 °C in NO/O_2 prior to the temperature ramp (□).

Figure 5(a). Displaced NO_x TPD profiles following a dose in NO/O_2 at 400 °C. Na-ZSM-5 (□), Fe Ba ZSM-5(ion exchanged)(●) Fe Ba ZSM-5(wet impregnated) (○), Ba-ZSM-5 (◇) and Fe-ZSM-5 (◆).

Figure 5(b): Histogram showing the total amount of NO_x desorbed (black), the NO_x desorbed during nitrite decomposition (hatched) and the NO_x desorbed during nitrate decomposition (white), from the various catalysts. (Na ZSM 100 refers to a sample of

Na ZSM which had been dosed in NO/O_2 at 100 °C, (ie) refers to an ion exchanged Ba catalyst and (wi) refers to a wet impregnated Ba catalyst).

Figure 6: Temperature Programmed Surface Reaction between $NO_{x\ ads}$ (catalysts dosed in NO/O_2 at 400 °C to 100 °C) and $NH_{3(g)}$. (a) FeZSM-5, (b) Ba-ZSM-5 (c) Fe Ba ZSM-5 (ion exchanged) (d) Fe Ba ZSM-5 (wet impregnated), NH_3 (❑), N_2 (○), NO (△), N_2O (◊).

Figure 7: Displaced NH_3 TPD profiles from each of the materials. The values in parentheses indicate the total amount of desorbed NH_3 in μmol g^{-1} of catalyst. Ba-ZSM-5 (◇) (913), Fe-ZSM-5 (◆) (1117), Na-ZSM-5 (□) (749), Fe Ba ZSM-5 (wet impregnated) (◦) (833) and Fe Ba ZSM-5 (ion exchanged) (•) (794).

Figure 8: Temperature Programmed Surface Reaction between $NH_{3\ ads}$ + $NO/O_{2\ (g)}$. (a) FeZSM-5, (b)Ba-ZSM-5 (c) Fe Ba ZSM-5 (ion exchanged) (d) Fe Ba ZSM-5 (wet impregnated), NH_3 (❑), N_2 (○), NO (△), N_2O (◊).

FIGURE 1

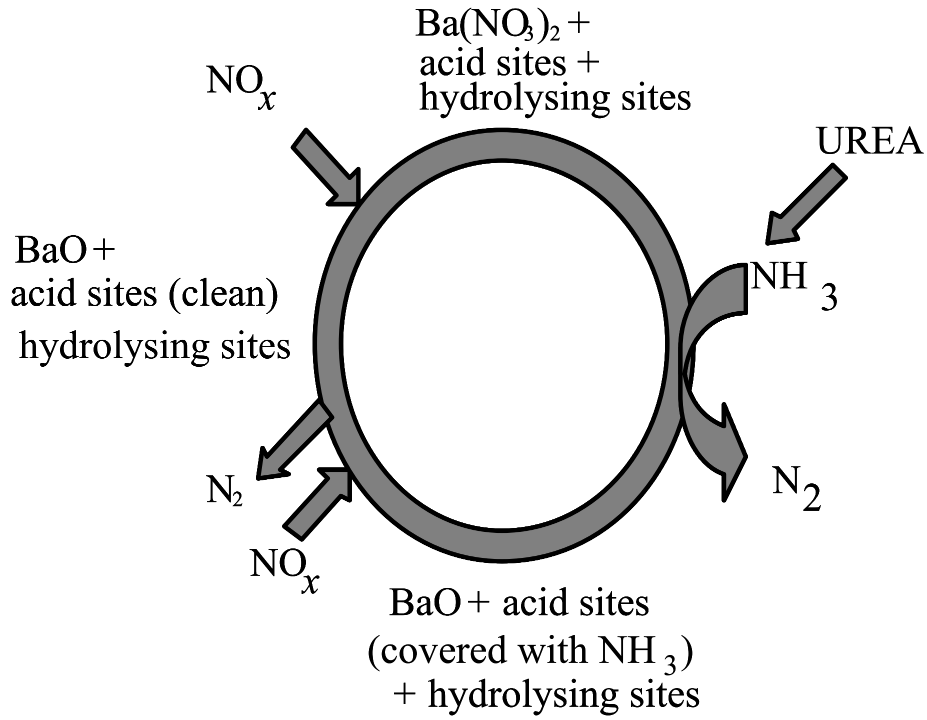

Ba(NO3)2 +
acid sites +
hydrolysing sites
NOx
UREA
BaO +
acid sites (clean)
hydrolysing sites
NH 3
N2
N2
NOx
BaO + acid sites
(covered with NH 3)
+ hydrolysing sites

FIGURE 2

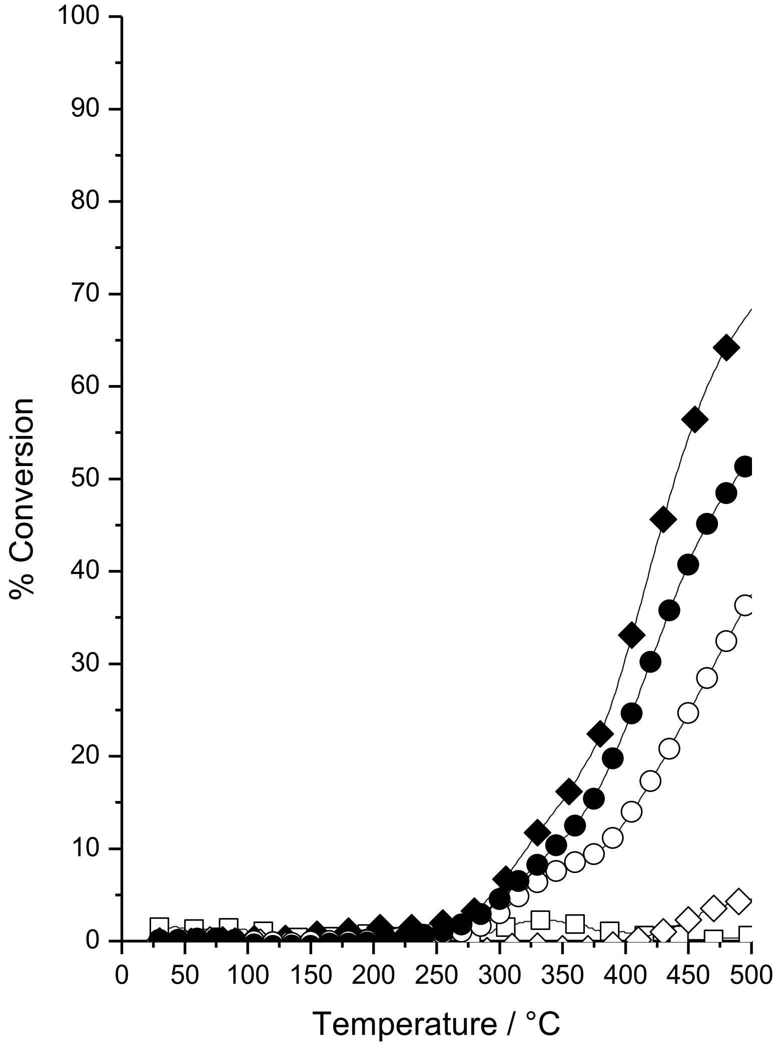

100
90
80
70
60
50
40
30
20
10
0
% Conversion
0
50
100
150
200
250
300
350
400
450
500
Temperature / °C

FIGURE 3

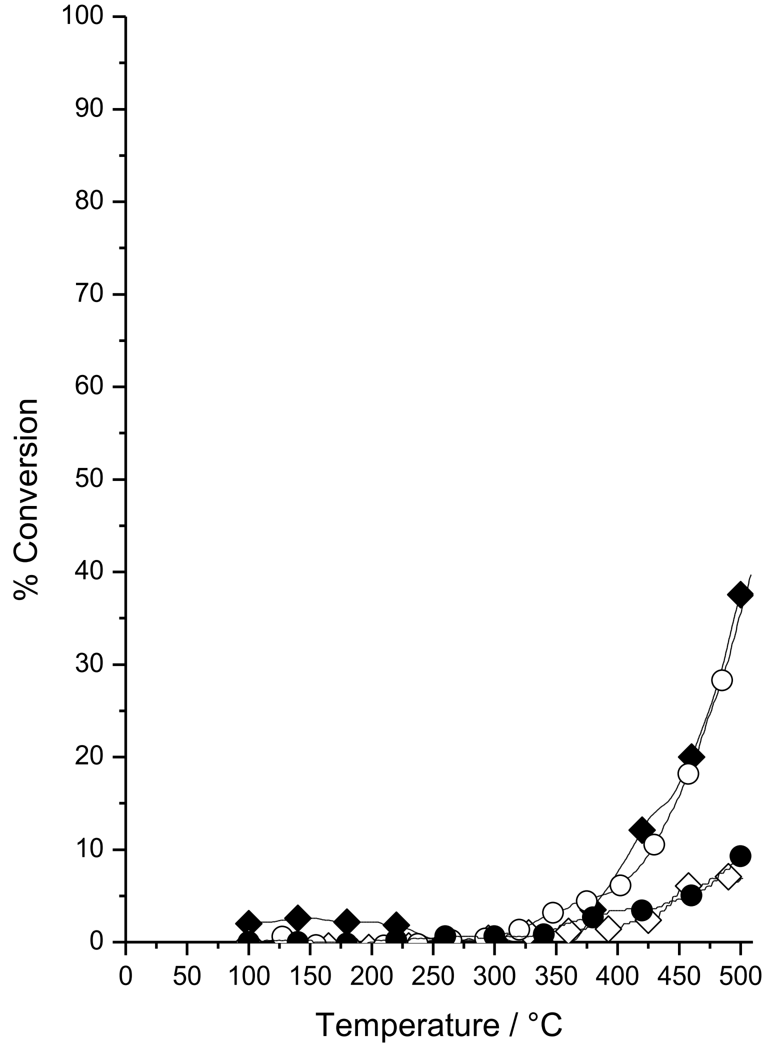

% Conversion
0
10
20
30
40
50
60
70
80
90
100
Temperature / °C
0
50
100
150
200
250
300
350
400
450
500

FIGURE 4

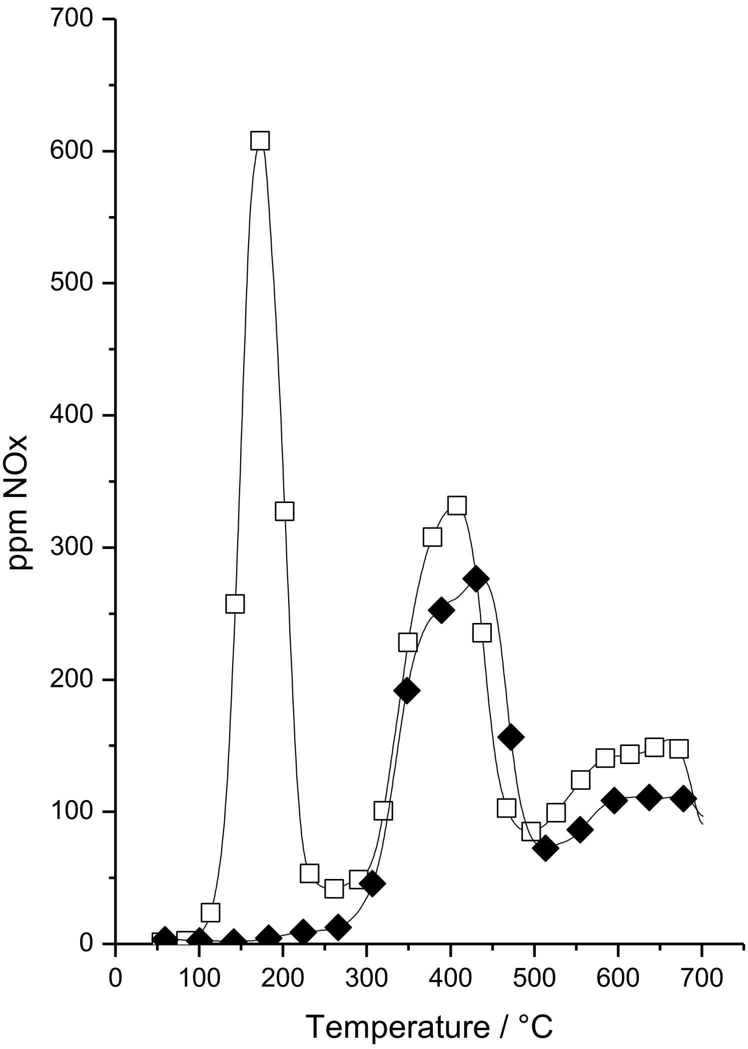
700
600
500
400
300
200
100
0
ppm NOx
0
100
200
300
400
500
600
700
Temperature / °C

FIGURE 5A5a

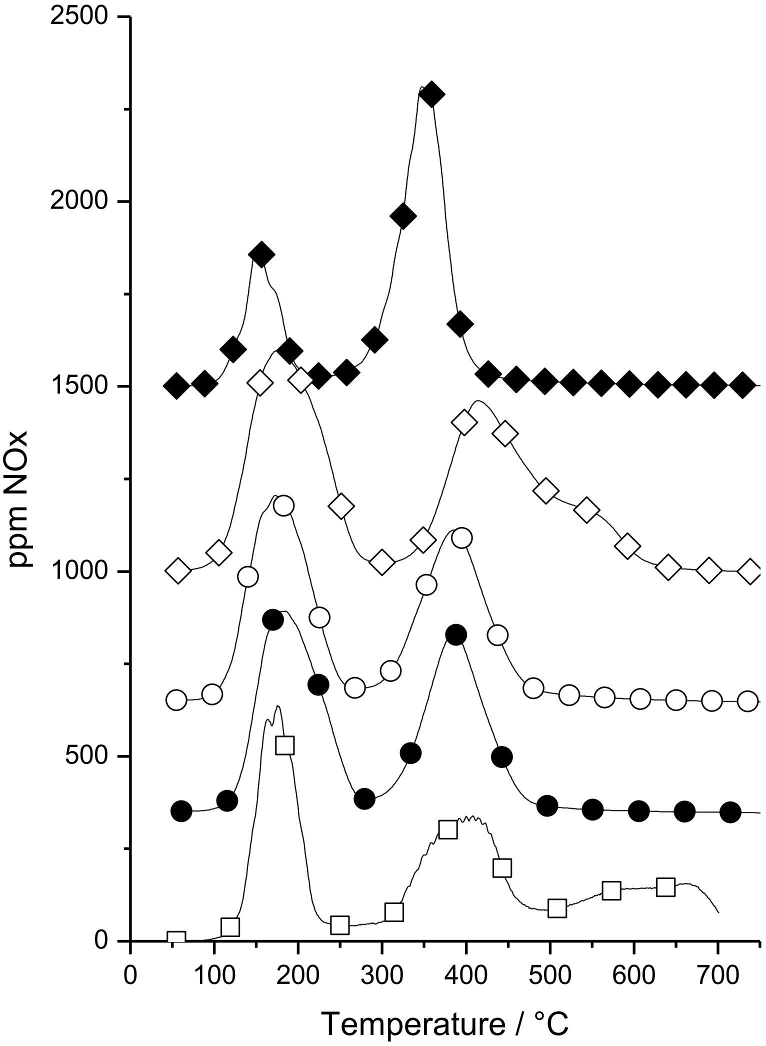

2500
2000
1500
1000
500
0
ppm NOx
0
100
200
300
400
500
600
700
Temperature / °C

FIGURE 5B5b

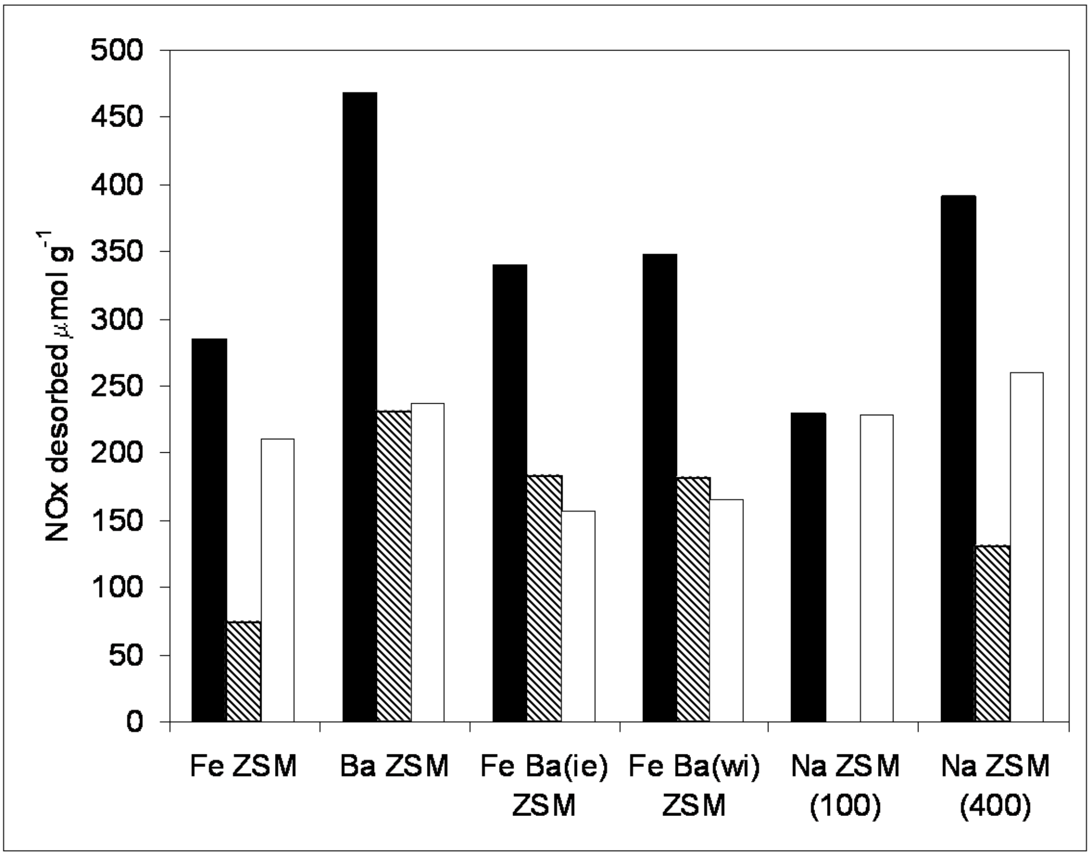

NOx desorbed μmol g^{-1}
500
450
400
350
300
250
200
150
100
50
0
Fe ZSM
Ba ZSM
Fe Ba(ie) ZSM
Fe Ba(wi) ZSM
Na ZSM (100)
Na ZSM (400)

FIGURE 6 a-d

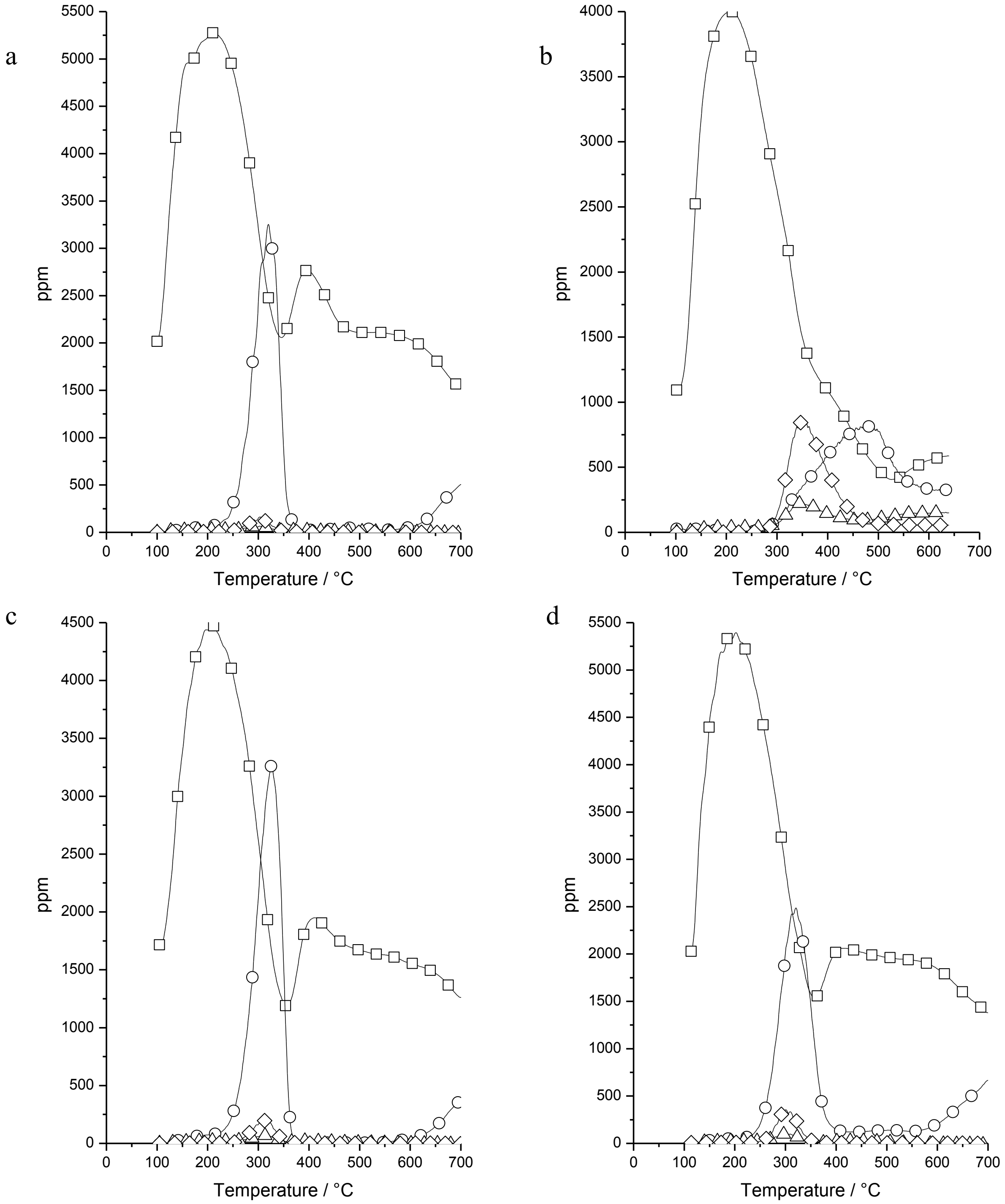

FIGURE 7

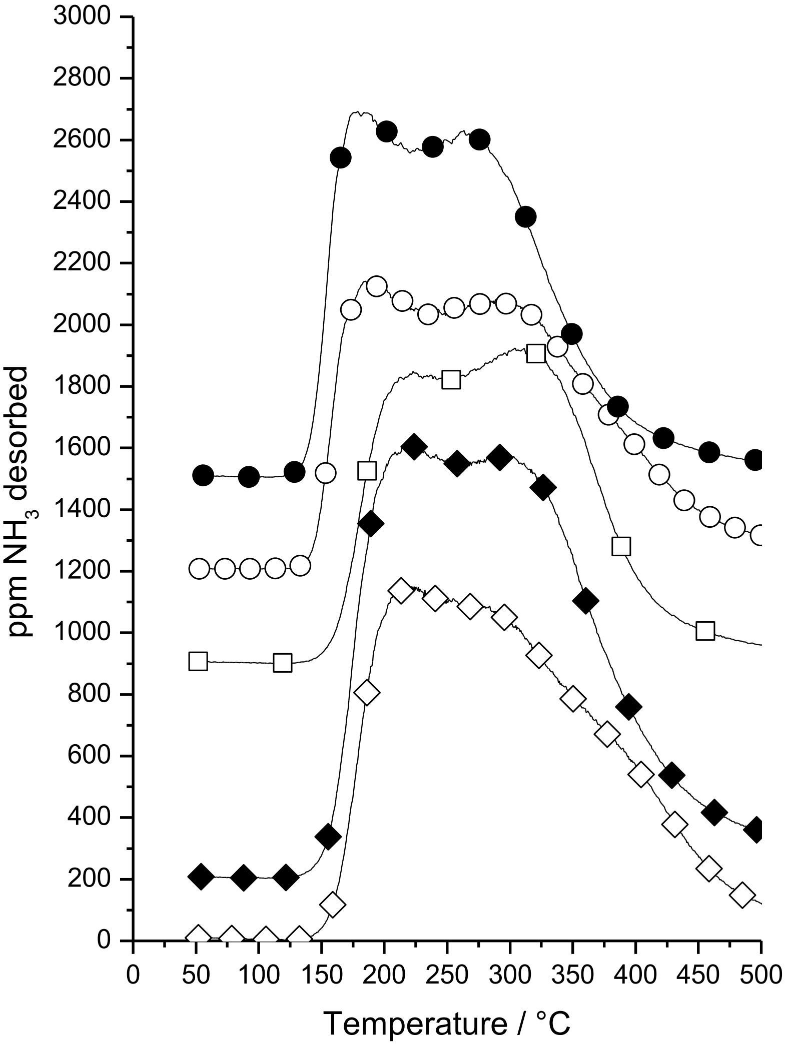

ppm NH_3 desorbed
Temperature / °C
0
50
100
150
200
250
300
350
400
450
500
200
400
600
800
1000
1200
1400
1600
1800
2000
2200
2400
2600
2800
3000

FIGURE 8 a-d

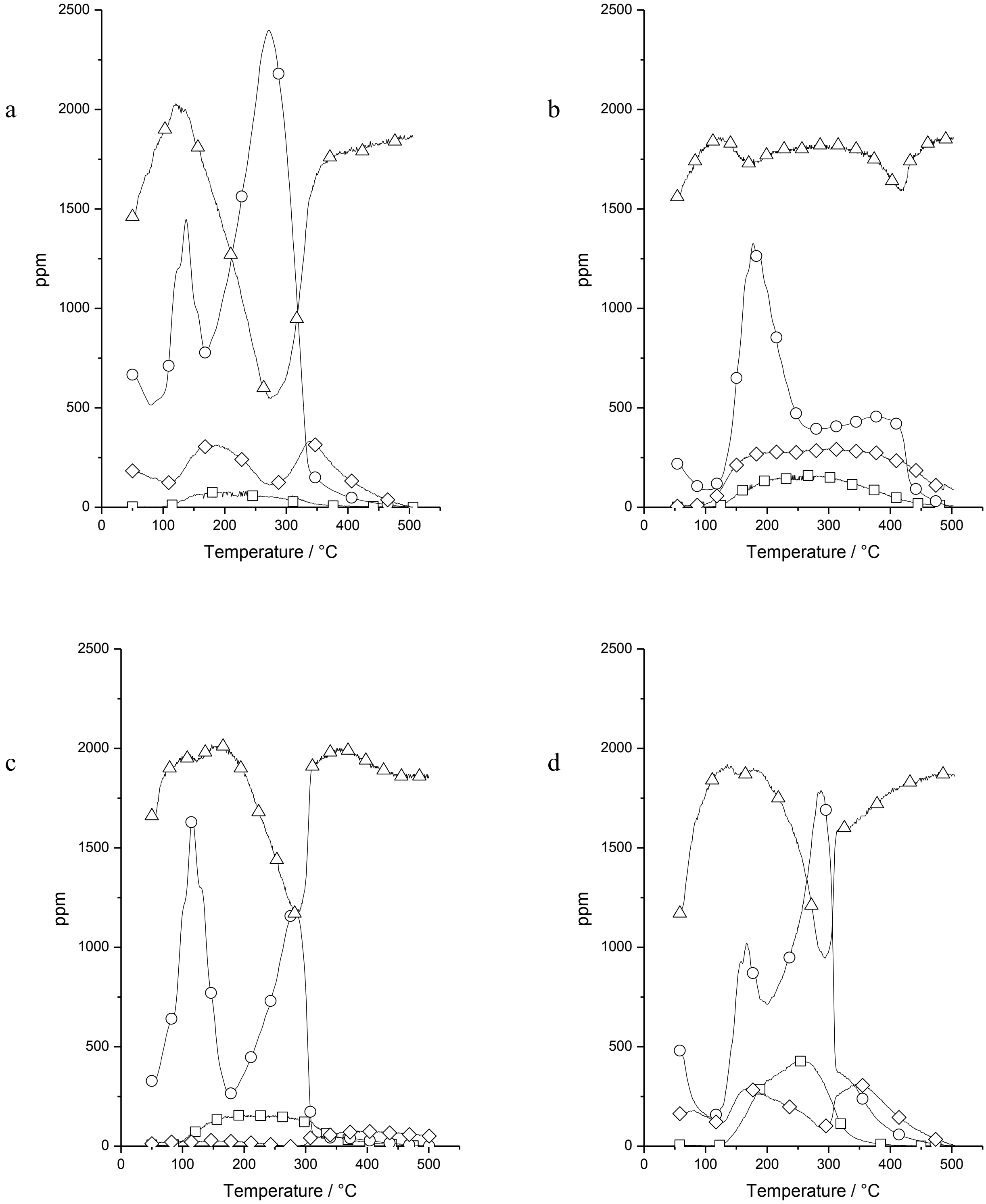
a
b
c
d
2500
2000
1500
1000
500
0
ppm
0
100
200
300
400
500
Temperature / °C